Aerotecnica Missili & Spazio (2024) 103:245–253
https://doi.org/10.1007/s42496-023-00193-2

ORIGINAL ARTICLE

Near-Optimal Feedback Guidance for Low-Thrust Earth Orbit Transfers

D. Atmaca[1] · **M. Pontani**[2]

Received: 16 September 2023 / Revised: 23 November 2023 / Accepted: 11 December 2023 / Published online: 1 February 2024

Abstract
This research describes a near-optimal feedback guidance, based on nonlinear orbit control, for low-thrust Earth orbit transfers. Lyapunov stability theory leads to proving that although several equilibria exist, only the desired operational conditions are associated with a stable equilibrium. This ensures quasi-global asymptotic convergence toward the desired final orbit. The dynamical model includes the effect of eclipsing on the available thrust, as well as all the relevant orbit perturbations, such as several harmonics of the geopotential, solar radiation pressure, aerodynamic drag, and gravitational attraction due to the Sun and the Moon. Near-optimality of the feedback guidance comes from careful selection of the control gains. They are identified in two steps. Step (a) is an extensive table search in which the gains are changed in a large interval. Step (b) uses a numerical optimization algorithm that refines the gains found in (a), while minimizing the time of flight. For the numerical simulations, two scenarios are defined: (i) nominal conditions and (ii) nonnominal conditions, which arise from orbit injection errors and stochastic failures of the propulsion system. For case (i), gain optimization leads to obtaining numerical results very close to those corresponding to a known optimal orbit transfer with eclipse arcs. Moreover, for case (ii), extensive Monte Carlo simulations demonstrate that the nonlinear feedback guidance at hand is effective in driving a spacecraft from a low Earth orbit to a geostationary orbit, also in the presence of nonnominal flight conditions.

Keywords Earth orbit transfers · Low-thrust space propulsion · Feedback guidance and control

1 Introduction

Orbit control is a crucial task in space missions and was extensively studied in the last decades. Many works focused on continuous-thrust and impulsive transfers, using optimal control theory. In recent years, near-optimal strategies are gaining increasing attention and relevance for spacecraft equipped with low-thrust propulsion systems, because similar approaches allow real-time compensation of orbital perturbations, while achieving satisfactory performance in terms of propellant consumption.

The study of nonlinear and near-optimal feedback guidance for low-thrust spacecraft is a relatively new topic, with significant publications appeared over the last 3 decades. An important contribution is due to Gurfil [1], who utilizes nonlinear control with classical orbit elements for low-thrust orbit transfers. His study addresses asymptotic convergence from an initial elliptical orbit to any final elliptical orbit using the Gauss variational equations. Recently, Pontani and Pustorino [2] used modified equinoctial elements, in conjunction with nonlinear control for orbit injection and maintenance. This approach takes advantage of Lyapunov stability combined with LaSalle's invariance principle. Gao [3] presents a linear feedback guidance technique that exhibits near-optimality for low-thrust Earth orbit transfers using orbital averaging. Kluever [4] proposed a simple closed-loop feedback-driven scheme for low-thrust orbit transfers that allows calculating sub-optimal trajectories. Petropoulos [5] developed a simple strategy based on candidate Lyapunov functions for low-thrust orbit transfers, while coining the term proximity quotient or Q-Law. There are several other studies based on Q-Law [6, 7], and they focus on mitigating the sub-optimality of this strategy.

✉ M. Pontani
mauro.pontani@uniroma1.it

D. Atmaca
d.atmaca@tudelft.nl

[1] Delft University of Technology, Kluyverweg 1, 2629 HS Delft, The Netherlands

[2] Department of Astronautical, Electrical, and Energy Engineering, Sapienza University of Rome, Via Salaria 851, 00138 Rome, Italy

This research proposes a near-optimal feedback guidance based on nonlinear control for low-thrust Earth orbit transfers. The dynamical system is modeled with the inclusion of the effect of the eclipse condition and all the relevant orbital perturbations, such as harmonics of geopotential, solar radiation pressure, aerodynamic drag, and gravitational attraction due to the Sun and the Moon. Near-optimality of the feedback guidance is sought from careful selection of the nonlinear control gains. To do this, a two-stage process for gain selection is being presented and tested. For the numerical simulations, two flight conditions are defined: (i) nominal conditions and (ii) nonnominal conditions that account for the orbit injection errors and the stochastic failures of the propulsion system. The nonnominal flight condition is studied through extensive Monte Carlo simulations, to demonstrate both numerical stability and the convergence properties of the nonlinear feedback guidance at hand. To illustrate the performance under both conditions, orbit transfers from different low Earth orbits (LEO) to the geostationary orbit (GEO) are considered. In a specific illustrative example, the initial and final orbit elements are taken from an existing study on optimal orbit control [8], for the purpose of showing near optimality of the nonlinear feedback guidance.

2 Orbit Dynamics

Orbit dynamics is described in suitable reference systems. The initial frame of interest is the Earth-centered inertial frame (ECI) identified by a right-hand sequence of unit vectors $(\hat{c}_1, \hat{c}_2, \hat{c}_3)$, where $\hat{c}_1$ is the vernal axis and $\hat{c}_3$ is aligned with the Earth rotation axis. The local-vertical-local-horizontal frame (LVLH) is associated with $(\hat{r}, \hat{\theta}, \hat{h})$, where $\hat{r}$ points toward the spacecraft position vector (taken from the center of the Earth), whereas $\hat{h}$ is directed along the specific angular momentum.

Orbit dynamics can be described with the use of osculating orbit elements, i.e., semimajor axis a, eccentricity e, inclination i, right ascension of the ascending node (RAAN) Ω, argument of periapse ω, and true anomaly θ_*. However, these elements lead to singularities in the Gauss planetary equations for circular and equatorial orbits. To avoid these issues, this study utilizes Modified Equinoctial Elements (MEE) [9], which avoid all singular conditions except in the occurrence of equatorial retrograde orbits. The definition of MEE is

$$\begin{array}{ccccc} p = a\left(1-e^2\right) & \cdots & l = e\cos(\Omega+\omega) & \cdots & m = e\sin(\Omega+\omega) \\ n = \tan\frac{i}{2}\cos\Omega & & s = \tan\frac{i}{2}\sin\Omega & & q = \Omega+\omega+\theta_*. \end{array} \tag{1}$$

It is convenient to express these in a compact form, by including 5 components in $\boldsymbol{z}$, accompanied by the respective governing equation,

$$\begin{aligned} \boldsymbol{z} &= \begin{bmatrix} x_1 & x_2 & x_3 & x_4 & x_5 \end{bmatrix}^T = \begin{bmatrix} p & l & m & n & s \end{bmatrix}^T \\ \dot{\boldsymbol{z}} &= \mathbf{G}(\boldsymbol{z}, x_6)\boldsymbol{a}. \end{aligned} \tag{2}$$

In Eq. (2), term $\boldsymbol{a}$ includes both perturbing and thrust accelerations acting on the spacecraft, whereas $\mathbf{G}(\boldsymbol{z}, x_6)$ is a matrix defined as

$$\mathbf{G}(\boldsymbol{z}, x_6) = \sqrt{\frac{x_1}{\mu_E}} \begin{bmatrix} 0 & \frac{2x_1}{\eta} & 0 \\ \sin x_6 & \frac{(\eta+1)\cos x_6 + x_2}{\eta} & -\frac{x_4 \sin x_6 - x_5 \cos x_6}{\eta} x_3 \\ -\cos x_6 & \frac{(\eta+1)\sin x_6 + x_3}{\eta} & \frac{x_4 \sin x_6 - x_5 \cos x_6}{\eta} x_2 \\ 0 & 0 & \frac{1+x_4^2+x_5^2}{2\eta}\cos x_6 \\ 0 & 0 & \frac{1+x_4^2+x_5^2}{2\eta}\sin x_6 \end{bmatrix}. \tag{3}$$

Letting $x_6 = q$, the related time derivative is

$$\begin{aligned} \dot{x}_6 = &\sqrt{\frac{\mu_E}{x_1^3}}\left(1 + x_2\cos x_6 + x_3 \sin x_6\right)^2 \\ &+ \sqrt{\frac{x_1}{\mu_E}} \frac{x_4 \sin x_6 - x_5 \cos x_6}{1 + x_2 \cos x_6 + x_3 \sin x_6} a_h, \end{aligned} \tag{4}$$

where a_h is the overall acceleration in the direction of angular momentum. From these definitions, some useful expressions can be identified, such as $r = p/\eta$, where r is the instantaneous orbital radius and $\eta = 1 + x_2 \cos x_6 + x_3 \sin x_6$.

This study assumes throttleable and steerable low thrust, with an upper bound $T_{\max}$ on the thrust magnitude and the assumption that propulsion is only available when the spacecraft is illuminated. Two parameters identify the performance of the propulsion system: (a) $u_T^{(\max)} = T_{\max}/m_0$, i.e., the ratio of the maximum thrust magnitude to initial mass m_0, and (b) c, which is the (constant) effective exhaust velocity. The following expressions characterize the mass ratio and its time derivative:

$$x_7 = \frac{m}{m_0} \quad \text{and} \quad \dot{x}_7 = -\frac{u_T}{c}, \tag{5}$$

where m is the mass at a generic time instant, and $\dot{x}_7$ identifies the mass ratio depletion rate. From these relations, $\boldsymbol{a}_T = \boldsymbol{u}_T/x_7$ represents the instantaneous thrust acceleration projected onto the LVLH frame, while $u_T = |\boldsymbol{u}_T|$ is constrained to the interval $\left[0, u_T^{(\max)}\right]$.

Expanding the $\boldsymbol{a}$ term in Eq. (2) yields $\boldsymbol{a} = \boldsymbol{a}_T + \boldsymbol{a}_P$, where $\boldsymbol{a}_P$ refers to the perturbing acceleration. For this study, four types of orbit perturbations are considered: (1) Earth gravitational harmonics (specifically, the harmonics with $|J_{l,m}| > 10^{-6}$ defined in the EGM2008 model [10], i.e., J_2, J_3, J_4, J_{31}, and J_{22}), (2) solar radiation pressure, (3) third-body attraction due to the Sun and the Moon, and (4) aerodynamic drag. The latter is modeled by assuming a reference surface area of 23.569 m^2 and ballistic coefficient

equal to $0.0576\,\mathrm{m}^2/\mathrm{kg}$. In addition, the solar radiation pressure is modeled using a fully reflective surface area, leading to a radiation pressure coefficient equal to 2. The assumed values for the reference surface, the ballistic coefficient, and the radiation pressure coefficient correspond to upper bounds for the respective perturbing accelerations, for the purpose of proving that nonlinear feedback control is effective even in the presence of moderate (overestimated) orbit perturbations.

The initial epoch for all simulations is March 20, 2025 at 0:00 UTC.

In short, $\boldsymbol{x} = \begin{bmatrix} z^T & x_6 & x_7 \end{bmatrix}^T = \begin{bmatrix} x_1 & x_2 & x_3 & x_4 & x_5 & x_6 & x_7 \end{bmatrix}^T$ identifies the complete state vector in compact form, whereas $\boldsymbol{u}_T$ is the control vector.

3 Nonlinear Orbit Control

The first goal of nonlinear orbit control is to identify a feedback law that can drive the spacecraft toward the desired orbit. Then, stability is studied through the fundamental principles of Lyapunov theory, under the assumption of perfect knowledge of the state. This also implies that noise and navigation errors are not considered in this study. In addition, a novel gain selection strategy for selecting the nonlinear control gains is proposed in this section.

3.1 Feedback Law and Stability Analysis

The following developments regarding the Lyapunov stability theory applied to nonlinear orbit control follow a recent paper by Pontani and Pustorino [2]. A target set is defined as $\boldsymbol{\psi}(z) = \boldsymbol{0}$. It is related to the desired final conditions. Because z only contains five elements, $\dim(\boldsymbol{\psi}) \leq 5$. Using the target set, the candidate Lyapunov function can be defined as

$$V = \frac{1}{2}\boldsymbol{\psi}^T \mathbf{K} \boldsymbol{\psi}, \tag{6}$$

where $\mathbf{K}$ is a diagonal, positive-definite matrix of gains. From Eq. (6), it is apparent that $V > 0$ and $V = 0$ only if $\boldsymbol{\psi} = \boldsymbol{0}$. The following propositions can be used to identify a suitable and effective feedback law.

Proposition 1: *Let* $b := \mathbf{G}^T(\partial\boldsymbol{\psi}/\partial z)^T\mathbf{K}\boldsymbol{\psi}$. *If* $\boldsymbol{\psi}$ *and* $(\partial\boldsymbol{\psi}/\partial z)$ *are continuous,* $|\boldsymbol{b}| > \boldsymbol{0}$ *unless* $\boldsymbol{\psi} = \boldsymbol{0}$ *and* $u_T^{(\max)} \geq \left|x_7(\boldsymbol{a}_P + \boldsymbol{b})\right|$, *then the feedback control law*

$$\boldsymbol{u}_T = -x_7(\boldsymbol{b} + \boldsymbol{a}_P) \tag{7}$$

leads to a dynamical system governed by Eqs. (2), (4) *and* (5) *to asymptotically converge to the target set associated with* $\boldsymbol{\psi}(z) = \boldsymbol{0}$.

Proposition 1 *leads to obtaining the following expression for the time derivative of* V:

$$\dot{V} = -\boldsymbol{b}^T\boldsymbol{b}, \quad \text{where} \quad \boldsymbol{b} = \mathbf{G}^T\left(\frac{\partial\boldsymbol{\psi}}{\partial z}\right)^T\mathbf{K}\boldsymbol{\psi}. \tag{8}$$

Therefore, the feedback law, $\boldsymbol{u}_T$, *is chosen in a way that makes* $\dot{V}$ *strictly negative except when* $\boldsymbol{b} = \boldsymbol{0}$, *forcing asymptotic convergence toward the target set. However, the preceding proposition is useful only if* $|\boldsymbol{u}_T| \leq u_T^{(\max)}$. *The following proposition addresses the saturation of the thrust magnitude.*

Proposition 2: *Let* $b := \mathbf{G}^T(\partial\boldsymbol{\psi}/\partial z)^T\mathbf{K}\boldsymbol{\psi}$. *If* $\boldsymbol{\psi}$ *and* $(\partial\boldsymbol{\psi}/\partial z)$ *are continuous,* $|\boldsymbol{b}| > 0$ *unless* $\boldsymbol{\psi} = \boldsymbol{0}$, $u_T^{(\max)} < x_7|b + a_P|$, *and* $b^T a_P \leq 0$ *then the feedback control law*

$$\boldsymbol{u}_T = -u_T^{(\max)}\frac{\boldsymbol{a}_P + \boldsymbol{b}}{|\boldsymbol{a}_P + \boldsymbol{b}|} \tag{9}$$

leads to a dynamical system governed by Eqs. (2), (4) *and* (5) *to asymptotically converge to the target set associated with* $\boldsymbol{\psi}(z) = \boldsymbol{0}$.

In real mission scenarios, the inequality $\boldsymbol{b}^T\boldsymbol{a}_P \leq 0$ *does not hold along the entire transfer path. Nevertheless, the following proposition provides an additional sufficient condition that guarantees convergence toward the target set.*

Proposition 3: *Let* $b := \mathbf{G}^T(\partial\boldsymbol{\psi}/\partial z)^T\mathbf{K}\boldsymbol{\psi}$. *If* $\boldsymbol{\psi}$ *and* $(\partial\boldsymbol{\psi}/\partial z)$ *are continuous,* $|\boldsymbol{b}| > 0$ *unless* $\boldsymbol{\psi} = \boldsymbol{0}$ *and* $x_7|\boldsymbol{a}_P| < u_T^{(\max)} < x_7|\boldsymbol{b} + \boldsymbol{a}_P|$ *then the feedback control law* (9) *leads to a dynamical system governed by Eqs.* (2), (4) *and* (5) *to asymptotically converge to the target set associated with* $\boldsymbol{\psi}(z) = \boldsymbol{0}$.

The feedback laws (7) *and Eq.* (9) *can be combined, to yield*

$$\boldsymbol{u}_T = -u_T^{(\max)}\frac{x_7(\boldsymbol{b} + \boldsymbol{a}_P)}{\max\left\{u_T^{(\max)}, \left|x_7(\boldsymbol{b} + \boldsymbol{a}_P)\right|\right\}}. \tag{10}$$

This final form of the feedback law ensures asymptotical stability and accounts for the limitations of the propulsion system. Also, it identifies a sufficient condition for stability, which dictates that the convergence to the final orbit is guaranteed if the thrust acceleration is larger than the perturbing acceleration. Because it identifies a sufficient condition for stability, local violations of this statement do not necessarily lead to instability of the entire system.

Once the feedback law is identified, the subsequent step consists of studying the stability properties referred to a specific target set. This paper considers the final operational orbit defined in terms of semilatus rectum, eccentricity, and inclination. Hence, the target set can be written as

$$\boldsymbol{\psi} = \begin{bmatrix} x_1 - p_d \\ x_2^2 + x_3^2 - e_d^2 \\ x_4^2 + x_5^2 - \tan^2 \frac{i_d}{2} \end{bmatrix} = \begin{bmatrix} \psi_1 \\ \psi_2 \\ \psi_3 \end{bmatrix} = \boldsymbol{0}, \tag{11}$$

where subscript d denotes the desired value of the respective variable. To study the stability of the desired conditions, the attracting set, associated with $\boldsymbol{b} = \boldsymbol{0}$*, must be identified. This set turns out to contain five different subsets* [11]:

(1) $x_1 = 0$ (rectilinear trajectories)
(2) $x_1 = p_d \;\; x_2^2 + x_3^2 = e_d^2 \;\; x_4^2 + x_5^2 = 0$ (equatorial elliptic orbits)
(3) $x_1 = p_d \;\; x_2^2 + x_3^2 = 0 \;\; x_4^2 + x_5^2 = \tan^2\left(i_d/2\right)$ (*circular orbits with inclination* i_d)
(4) $x_1 = p_d x_2^2 + x_3^2 = 0 x_4^2 + x_5^2 = 0$ (equatorial circular orbits)
(5) $x_1 = p_d \;\; x_2^2 + x_3^2 = e_d^2 \;\; x_4^2 + x_5^2 = \tan^2\left(i_d/2\right)$ (target set).

Because the attracting set includes several subsets, the Lyapunov's stability theorem states that the convergence to the desired conditions is only local. However, using the Lyapunov method and LaSalle's invariance principle [12] *subset* 1 *can be ruled out* [11].

Furthermore, while subset 5 *is associated with the global minimum of V, the subsets* 2 *and* 3 *correspond to saddle points, whereas subset* 4 *is associated with a local maximum for V. In conclusion, even though subsets* 2–5 *are equilibrium conditions, numerical convergence occurs toward the target set* 5*, and the feedback law* (11) *guarantees quasi-global asymptotic stability for the dynamical system at hand.*

3.2 Gain Selection

Near-optimality of the feedback guidance comes from the gain optimization process described in this section. Since the target set has three components, the gain matrix $\mathbf{K}$ is a (3×3)-matrix. It is straightforward to notice that k_1 is related to the semilatus rectum, k_2 to eccentricity, and k_3 to the inclination

$$\mathbf{K} = \begin{bmatrix} k_1 & 0 & 0 \\ 0 & k_2 & 0 \\ 0 & 0 & k_3 \end{bmatrix}. \tag{12}$$

The gain selection method includes two sequential steps:

Step 1. Extensive table search that includes different gain combinations; each gain is changed with increment by $10^{0.1}$, in the interval $k_i = [1, 10^6]$.

Step 2. Using the values found at step 1, the native "*fminsearch*" MATLAB routine is utilized.

Step 2 refines the final values calculated at step 1 while minimizing the time of flight. To illustrate the gain selection method, the preceding two steps are completed for different initial orbits, associated with identical values of semimajor axis, eccentricity, RAAN, and argument of perigee, and different initial inclinations (cf. Table 1). The propulsion parameters for the gain optimization process are assumed to be $c = 30$ km/s and $u_T^{(\max)} = 10^{-4} g_0$, with $g_0 = 9.8065$ m/s^2. These values correspond to the performance available from the current technology [13]. The dynamical model for the gain selection only considers the J_2 harmonics of the Earth as the perturbing action, which is a valid assumption, since this is the dominant perturbation for low- and medium-altitude Earth orbits.

The gain values found at step 1 are reported in Table 2. The best case is identified after using different combinations of gains. It is found that the best performance corresponds to $k_1 = 1$ and $k_2 = k_3$. The final gain values, yielded by the

Table 1 Initial and final orbit elements; $i_0 = \{5°, 10°, 20°, 30°, 40°\}$

	a (km)	e	i (deg)	Ω (deg)	ω (deg)
Initial orbit	6778	0	i_0	0	–
Final orbit	42,164	0	0	–	–

Table 2 Gain values for step 1, with the associated transfer time and final mass ratios

i_0 (deg)	k_1	k_2	k_3	t_{sim} (days)	x_7
5	1	$10^{5.1}$	$10^{5.1}$	52.07	0.8529
10	1	$10^{4.4}$	$10^{4.4}$	54.74	0.8454
20	1	$10^{3.5}$	$10^{3.5}$	61.49	0.8263
30	1	$10^{3.0}$	$10^{3.0}$	68.26	0.8072
40	1	$10^{2.7}$	$10^{2.7}$	75.85	0.7858

Table 3 Optimized gain values, with the associated transfer time and final mass ratios

i_0 (deg)	k_1	k_2	k_3	t_{sim} (days)	x_7
5	1.0908	126,679	119,132	51.88	0.8535
10	0.9949	25,577	24,945	54.72	0.8454
20	0.9993	3164	3317	61.07	0.8275
30	0.9722	1056	967	68.19	0.8074
40	1.0261	515	502	75.76	0.7860

numerical optimization algorithm, are reported in Table 3. From its inspection it is apparent that k_1 remains very close to 1; instead, k_2 and k_3 undergo exponential decay as the initial inclination increases.

Comparison of Tables 2 and 3 indicates that while most of the optimized gain values provide improvement for the objective (i.e., the time of flight), some values in Table 3 remain very close to the respective values in Table 2.

4 Example of LEO–GEO Orbit Transfer

This section is focused on a specific LEO–GEO orbit transfer, for which the minimum-time solution (with eclipse arcs) is known from the scientific literature [8].

The near-optimal feedback guidance proposed in this study is tested under nominal and nonnominal conditions. For both cases, initial and final orbit elements, as well as the propulsion parameters, are taken from the existing study in Ref. [8]. The final orbit is the same as in Table 1, where the initial circular orbit is associated with $a_0 = 6927$ km and $i_0 = 28.5°$ (while the remaining elements are those reported in Table 1). The propulsion parameters are $c = 32.361$ km/s and $u_T^{(\max)} = 3.348 \cdot 10^{-4}$ m/s^2, and they characterize a low-thrust propulsion system. These propulsion values equal those used to get the optimal solution [8].

A significant advantage of the gain selection procedure is that once an optimized table of gains is identified, gains from this table can be used, even for different orbit transfer problems, with a variety of initial conditions and propulsion parameters. For the present illustrative example, the gains are chosen from Table 3 as $k_1 = 0.9722$, $k_2 = 1056$, and $k_3 = 967$. These gains refer to $i_0 = 30°$, which is the case closest to the initial inclination assumed in this section. In addition, the dynamical model includes all the previously listed orbit perturbations, as well as the effect of eclipsing on the available thrust. The following inequalities are used to identify the transfer time and final mass ratio at the end of the transfer:

$$|p - p_d| \leq 10 \text{ km} \qquad e \leq 0.005 \qquad i \leq 0.5°. \tag{13}$$

Table 4 Time of flight and final mass ratio for the illustrative example, using either optimal or feedback control

	Optimal control (no perturbation)	Feedback control (no perturbation)	Feedback control (with perturbations)
t_f (days)	215.94	235.84	228.22
$x_{7,f}$	0.8394	0.8241	0.8245

4.1 Numerical Results in Nominal Conditions

This subsection reports the numerical results under nominal conditions, with spacecraft eclipsing, either in the absence or in the presence of orbit perturbations. The results are compared to the minimum-time optimal transfer (cf. Table 4). Inspection of Table 4 reveals that the final mass ratio obtained with the feedback control law is very close to that corresponding to the optimal solution, whereas the time of flight differs by several days. Figure 1 shows the spacecraft trajectory in the ECI-frame, whereas Fig. 2 depicts the main orbit elements of interest. The insets in Fig. 2 show the oscillations due to the perturbations dominating the orbit dynamics under eclipse. In fact, because the thrust acceleration is unavailable during eclipse arcs, the natural orbit dynamics yields oscillations in the orbit elements. Figure 3 illustrates the time histories of the perturbing and thrust accelerations. At the beginning of the transfer, the magnitude of the perturbing acceleration is greater than that of the thrust acceleration. However, the perturbing term quickly decays to low values, mainly due to the decreasing effect of the Earth gravitational harmonics as the orbital radius increases.

Moreover, it is worth noting the effect of variable thrust at the end of the thrust acceleration plot. Because the desired

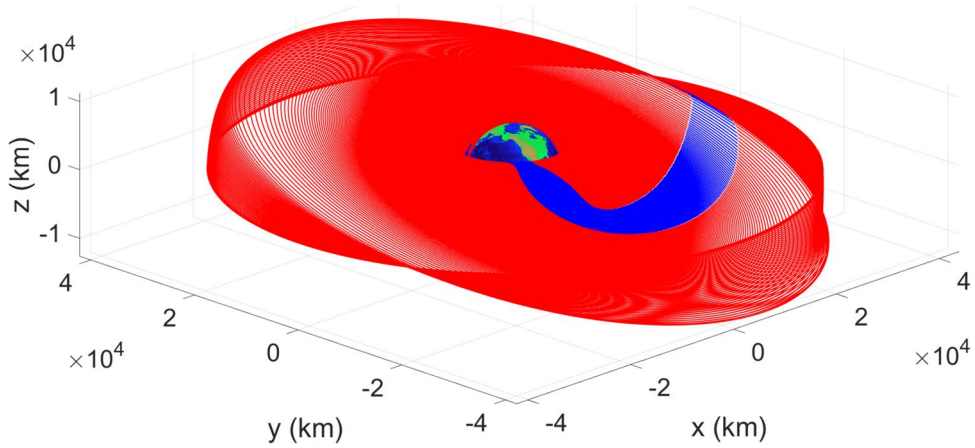

Fig. 1 Orbit transfer in the ECI-frame (blue arcs indicate eclipse)

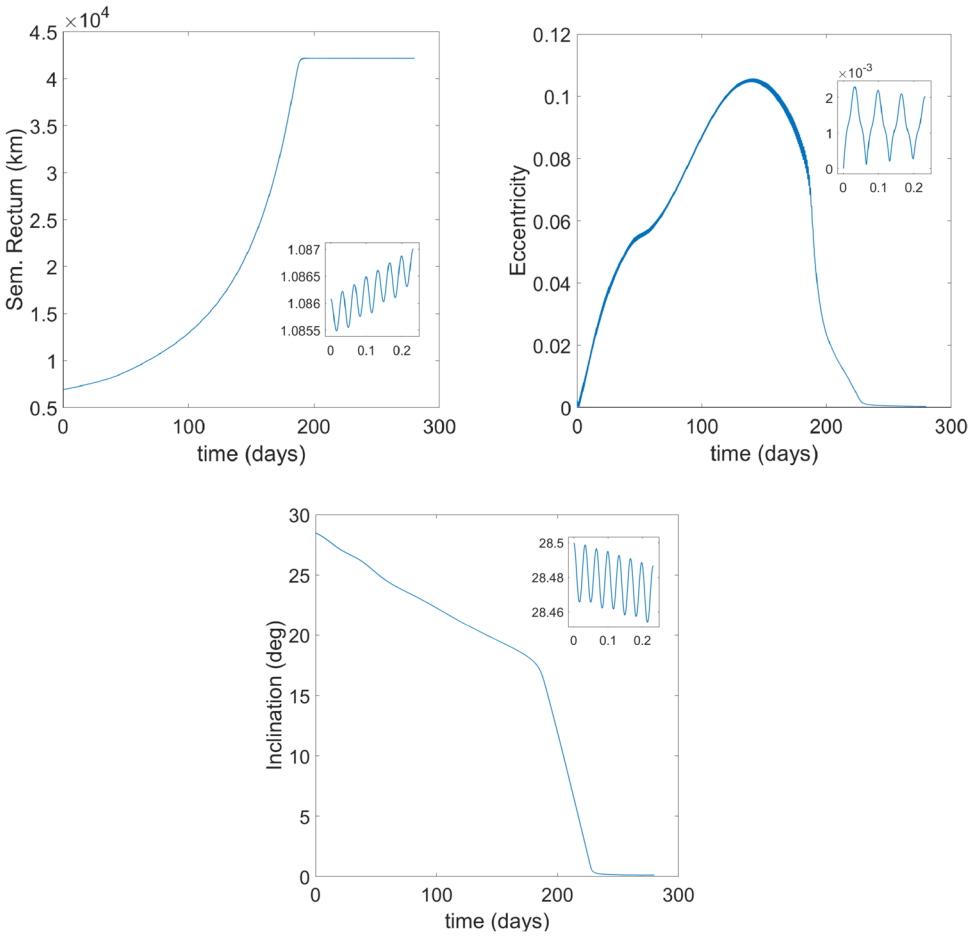

Fig. 2 Time histories of the main orbit elements of interest

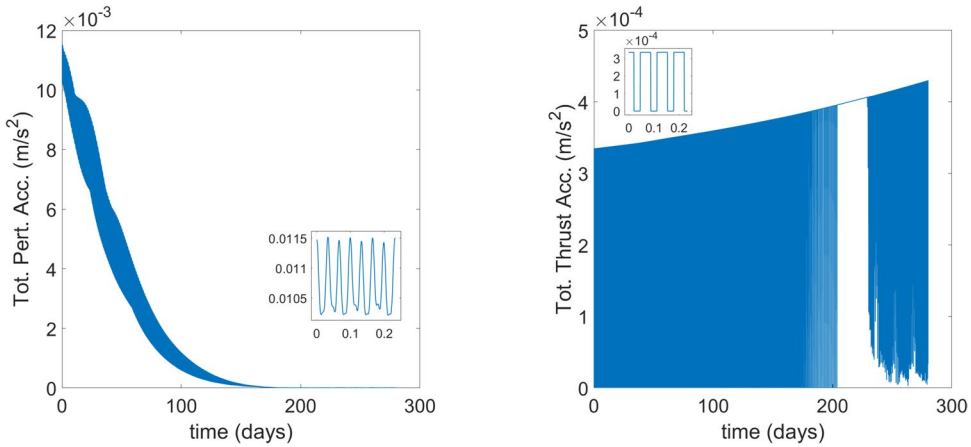

Fig. 3 Time histories of the total perturbing and thrust accelerations

orbit elements are close to the desired final values and the perturbing acceleration is much lower than the thrust acceleration in this phase, thrust acceleration is time-varying and is ignited for the purpose of orbit maintenance. If only discrete thrust levels were available, then suitable modulation schemes would be required, e.g., pulse width modulation or the multiple-level modulation addressed in Ref. [14]. However, this study assumes throttleable thrust, as mentioned in Sect. 2. Figure 4 portrays the time histories of the mass ratio, related to the propellant expenditure, and the Lyapunov function. From the inset of the mass ratio time history, one can notice that constant regions, associated with eclipse arcs, separate the regions where the mass ratio drops. In addition, even though the Lyapunov function starts from a positive value and globally decreases, the value locally increases. However, this increase does not lead to instability,

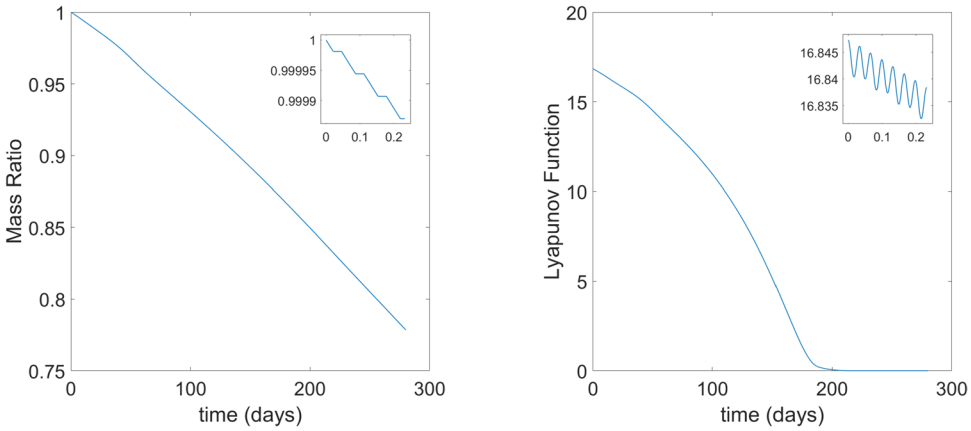

Fig. 4 Time histories of the mass ratio and the Lyapunov function

since the feedback law proposed in this study only provides a sufficient condition for stability. Hence, this demonstrates that the nonlinear feedback strategy can generate solutions that are close to the optimal transfer. In conclusion, nonlinear feedback guidance can be considered as an option alternative to optimal strategies in problems where real-time compensation of orbit perturbations is required.

4.2 Monte Carlo Analysis

This subsection focuses on nonnominal flight conditions, which account for the orbit injection errors and the stochastic failures of the propulsion system. The propulsion parameters, initial and final orbits, and gain values are identical to those in the nominal case. However, possible orbit injection errors may occur, and they are modeled through randomization of the initial orbit elements. First, the initial perigee and apogee radii are uniformly distributed in their respective intervals as

$$r_p \in [350, 549]\ \text{km} + R_E \quad \text{and} \quad r_a \in [549, 750]\ \text{km} + R_E, \tag{14}$$

where r_p is the perigee radius, r_a is the apogee radius, and R_E denotes the Earth radius. The semimajor axis and eccentricity are easily found from r_p and r_a. Moreover, the initial inclination has uniform distribution in [22.5, 34.5] deg. Finally, the remaining orbit elements are uniformly distributed, as follows:

$$\Omega \in [-\pi, \pi] \quad \omega \in [-\pi, \pi] \quad \theta_* \in [-\pi, \pi]. \tag{15}$$

The stochastic failures of the propulsion system are defined through two parameters: (i) starting point t_{fail} and (ii) duration t_{dur}. Once again, these obey a uniform distribution, with intervals [1, 100] days and [5, 20] days, respectively. Using these definitions, a Monte Carlo campaign composed of 1000 simulations is performed. Figure 5 shows all the orbit elements of interest. The insets of each figure refer to the first simulation and represent the interval when the stochastic failure occurs.

Even though the initial conditions are uniformly distributed and stochastic propulsion failure occurs, the feedback control successfully drives the spacecraft to the desired orbit. Table 5 reports the results and compares the proposed feedback guidance and the existing optimal solution. Comparing the results of the Monte Carlo Analysis with the nominal solution reveals a 3.59% increase in transfer time and a 0.13% decrease in the final mass ratio. In the end, the nonlinear feedback strategy is effective and only implies a modest performance penalty, in terms of time of flight. Although the latter is the objective to minimize, it is worth noting that the final mass ratio found with nonlinear orbit control is very close to that obtained through optimal control.

5 Concluding Remarks

This paper proposes and applies a recently introduced near-optimal feedback guidance strategy with gain tuning, to perform low-thrust Earth orbit transfers. The feedback law considers the thrust saturation, and is proven to enjoy quasi-global stability properties, under certain conditions. More specifically, the stability analysis, based on Lyapunov stability theory and the LaSalle's invariance principle, leads to identifying the attracting set, composed of five subsets, including the target set. However, the target set is demonstrated to be the only subset associated with a stable equilibrium. A novel, two-step gain selection strategy is developed to achieve near-optimality. The first step (a) is an exhaustive table search where the gains are incrementally changed in a large interval, using different combinations. The second step (b) is a numerical refinement process that tweaks the gain values found in (a) to minimize the time of flight. Effectiveness of the gain selection and the stability of the feedback law are numerically tested, with reference to an existing minimum-time

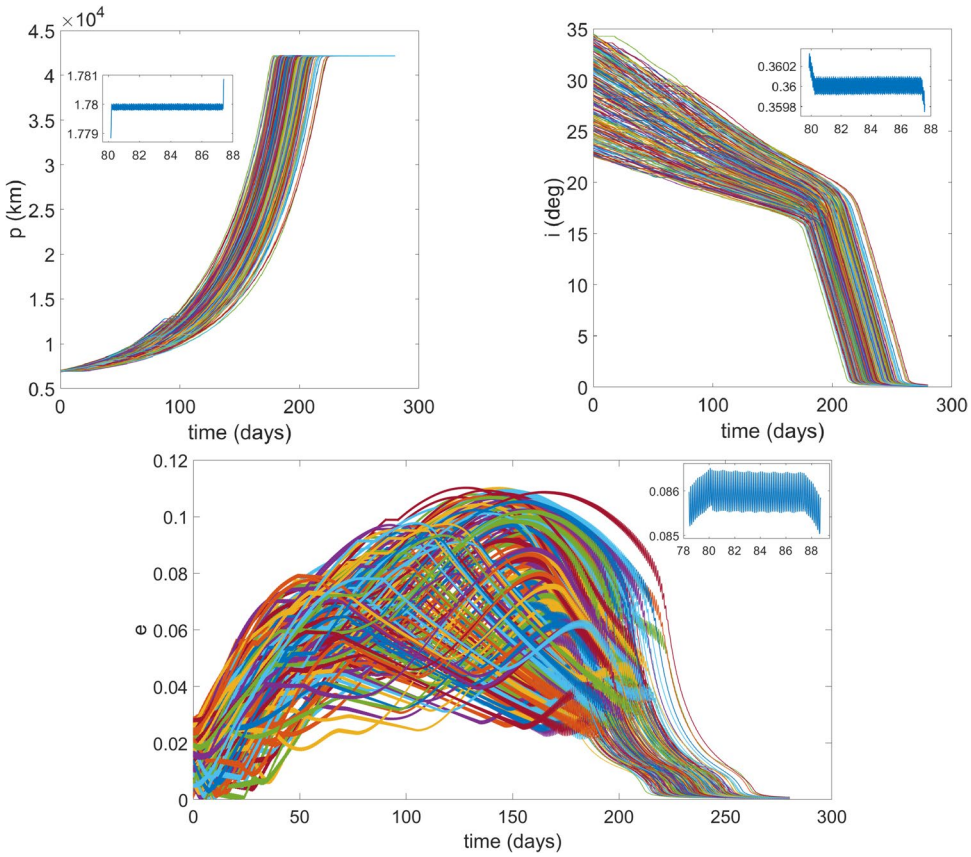

Fig. 5 Time evolution of some orbit elements of interest (Monte Carlo analysis)

Table 5 Statistical results of the Monte Carlo analysis and comparison with the optimal solution

	Mean	Standard deviation	Optimal solution
t_f(days)	236.41	10.5069	215.94
x_7	0.8234	0.0063	0.8394

solution coming from numerical optimization. Two different flight conditions are assumed: (i) nominal conditions and (ii) nonnominal conditions, which originate from orbit injection errors and stochastic failures of the propulsion system. In the numerical simulations, orbital perturbations and spacecraft eclipsing are modeled. Nonnominal conditions are studied through an extensive Monte Carlo Analysis, composed of 1000 simulations. The results point out that the feedback law is stable, even in the presence of nonnominal stochastic conditions. Moreover, the numerical results are also compared to the optimal solution reported in the literature. In conclusion, the nonlinear feedback strategy proposed in this work turns out to be effective and only implies a modest performance penalty with respect to the optimal solution.

Funding Open access funding provided by Università degli Studi di Roma La Sapienza within the CRUI-CARE Agreement.

Declarations

Conflict of Interest On behalf of all authors, the corresponding author states that there is no conflict of interest.

References

1. Gurfil, P.: Nonlinear feedback control of low-thrust orbital transfer in a central gravitational field. Acta Astronaut. **60**(8 & 9), 631–648 (2007)
2. Pontani, M., Pustorino, M.: Nonlinear earth orbit control using low-thrust propulsion. Acta Astronaut. **179**, 296–310 (2021)
3. Gao, Y.: Linear feedback guidance for low-thrust many-revolution earth-orbit transfers. J. Spacecr. Rocket. **46**(6), 1320–1325 (2009)
4. Kluever, C.A.: Simple guidance scheme for low-thrust orbit transfers. J. Guid. Control. Dyn. **21**(6), 1015–1017 (1998)
5. Petropoulos, A. E.: Low-thrust orbit transfers using candidate Lyapunov functions with a mechanism for coasting. In: AIAA/AAS Astrodynamics Specialist Conference and Exhibit, Rhode Island (2004)
6. Jagannatha, B.B., Bouvier, J.-B.H., Ho, K.: Preliminary design of low-energy, low-thrust transfers to halo orbits using feedback control. J. Guid. Control. Dyn. **42**(2), 1–12 (2018)
7. Holt, H., Armellin, R., Scorsoglio, A., Furfaro R.: Low-thrust trajectory design using closed-loop feedback-driven control laws and state-dependent parameters. In: AIAA Scitech 2020 Forum, Orlando (2020)
8. Pontani, M., Corallo, F.: Optimal low-thrust orbit transfers with shadowing effect using a multiple-arc formulation. In: 72nd International Astronautical Congress, Dubai (2021)
9. Walker, M.J.H., Ireland, B., Owens, J.: A set of modified equinoctial orbit elements. Celest. Mech. **36**(4), 409 (1985)
10. Palvis, N.K., Holmes, S.A., Kenyon, S.C., Factor, J.K.: An Earth gravitational model to degree 2160: EGM2008. In: General Assembly of the European Geosciences Union, Vienna (2008)
11. Pontani, M., Pustorino, M.: Low-thrust lunar capture leveraging nonlinear orbit control. J. Astronaut. Sci. **70**(5), 28 (2023)
12. Sastry, S.: Nonlinear Systems, Analysis, Stability, and Control, pp. 182–235. Springer, New York (1999)
13. Herman, A.L., Conway, B.A.: Optimal low-thrust Earth–Moon orbit transfer. J. Guid. Control. Dyn. **21**(1), 141–146 (1998)
14. Napoli, I., Pontani, M.: Discrete-variable-thrust guidance for orbital rendezvous based on feedback linearization. Aerotec. Missili Spaz. **101**, 351–360 (2022)